

## Photophysical characterization of *trans*-4,4'-disubstituted stilbenes

Vladislav Papper, Dina Pines, Gertz Likhtenshtein\*, Ehud Pines

Department of Chemistry, Ben-Gurion University of the Negev, P.O.B. 653, Beer-Sheva 84105, Israel

Received 17 April 1997; revised version received 15 July 1997; accepted 5 August 1997

### Abstract

Absorption and emission spectra of twenty *trans*-4,4'-disubstituted stilbenes have been measured in four solvents: cyclohexane (CH), chlorobenzene (CB), 2-butanone (methyl ethyl ketone, MEK) and dimethylsulfoxide (DMSO) at room temperature. Fluorescence quantum yields ( $\Phi_f$ ) and fluorescence lifetimes ( $\tau_f$ ) have been measured for these stilbenes. The lifetimes and quantum yields of fluorescence were found to be dependent on the donor–acceptor properties of the substituents and correlate with the Hammett  $\sigma$ -constants. In addition, we experimentally observed the appearance of a second emitting state which is close energetically to the lowest excited singlet state  $^1t^*$  in cases of strong donor–acceptor substituents in polar solvents. © 1997 Elsevier Science S.A.

**Keywords:** *Trans*-4,4'-disubstituted stilbenes; Photophysical characterization; Fluorescence quantum yields; Fluorescence lifetimes

### 1. Introduction

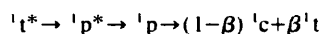
Photoisomerization has been known for several decades to dominate the photophysics of *trans*-stilbenes. It has been studied extensively and reviewed [1–12]. The chemistry of stilbene derivatives is straightforward, which allows the synthesis of many functional derivatives. We have prepared twenty *trans*-4,4'-disubstituted stilbenes in order to tune the reactant's properties over a wide range of reactivities. This enabled us to carry out a comprehensive study of the effect of the substituents on stilbene reactivity.

The photochemical behavior of stilbenes may be varied by the introduction of substituents which affect the charge distribution of the molecule. We have chosen the *para*-(4,4')-substituted stilbenes for our investigation of the electronic effects of the substituents on the photoisomerization reaction, because substitution in the *meta* (3,3',5,5')-ring positions has little effect on the course of the *trans*–*cis* photoisomerization process, i.e. the distinct conformers have similar spectra and fluorescence parameters. Substitution in the *ortho* (2,2',6,6')-positions introduces significant steric hindrance, causing the phenyl rings to twist out of plane about the double bond and changes the absorption and fluorescence spectral features.

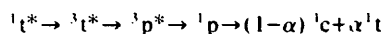
Solvent effects are also important in determining the reactivity of *trans*-4,4'-disubstituted stilbenes resulting from their dipolar characters. However, these effects are not extensively

studied in the present work and are the subject of our further research with a larger database.

It is generally accepted that the light-induced reversible isomerization of *trans*-stilbene [1–4] (Fig. 1) proceeds either from the lowest excited singlet state  $^1t^*$  through the twisted singlet intermediate  $^1p^*$  ('phantom' state):



or, alternatively, by the intersystem crossing pathway (ISC) through the biradical twisted triplet state  $^3p^*$ :



Here,  $^3t^*$  and  $^3p^*$  respectively are the *trans* and twisted configurations (perpendicular with respect to the C=C double bond) of the lowest triplet,  $^1p$  is the twisted ground state,  $(1-\alpha)$  is the fraction of triplet decay into the *cis*-form and  $(1-\beta)$  is the fraction of perpendicular singlet configuration decaying into the *cis*-form.

Usually, within a reaction series the functional correlation between substituent or solvent parameters and various substituent or solvent dependent rate processes is in the form of a linear Gibbs free-energy relationship [13]. To establish a reaction series we have introduced small changes on the reaction rate in two ways.

1. Modification of the stilbene molecule by introducing different donor–acceptor substituents. This leads to a Hammett-like behavior [14]. Although linear free-energy relationships usually deal with relative reactivities, in the form of reaction rate and equilibrium data, this approach

\* Corresponding author.

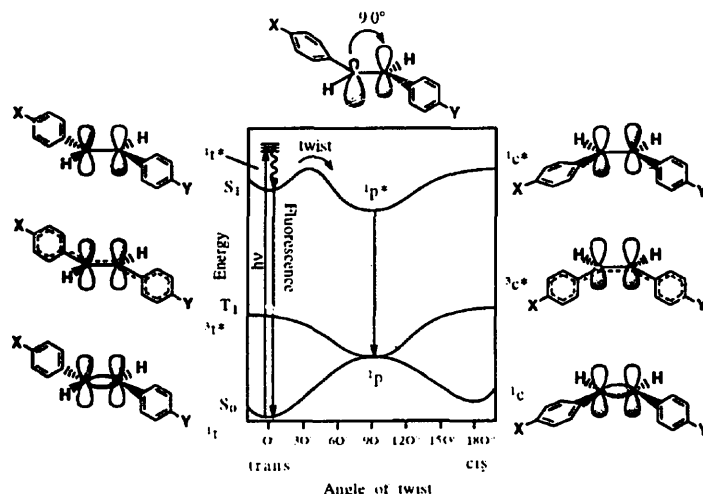
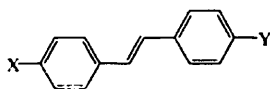


Fig. 1. Pictorial representation of the *trans* and *cis*-stilbene orbitals and electronic states participating in the *trans-cis* photoisomerization processes. The reaction coordinate is the torsional angle ( $\theta$ ) about the olefinic double bond.  $1t$  and  $1t^*$  are the ground state and the lowest excited singlet state of the *trans*-stilbene respectively.  $1p^*$  is the twisted singlet intermediate ('phantom' state).  $1c$  is the *trans*-configuration of the lowest triplet.  $1c$  and  $1c^*$  are the ground state and the lowest excited singlet state of the *cis*-stilbene respectively.  $3c^*$  is the *cis*-configuration of the lowest triplet.  $S_0$ ,  $S_1$  and  $T_1$  designate the potential energy surfaces of the ground singlet, first excited singlet and triplet states respectively.

Table 1  
Reaction yield, crystallization solvent and melting point of *trans*-4,4'-disubstituted stilbenes



	X	Y	Yield (%)	Crystallization solvent	Melting point (°C)	Reference
1	(CH <sub>3</sub> ) <sub>2</sub> N	Br	76	Toluene	232–234	[15]
2	(CH <sub>3</sub> ) <sub>2</sub> N	CN	70	1,4-Dioxane	250–251	[16]
3	(CH <sub>3</sub> ) <sub>2</sub> N	NH <sub>2</sub>	75	—	176	[17]
4	(CH <sub>3</sub> ) <sub>2</sub> N	Cl	43	Chlorobenzene	219–220	[17]
5	(CH <sub>3</sub> ) <sub>2</sub> N	OCH <sub>3</sub>	68	Acetone/isopropanol	185–186	[15]
6	(CH <sub>3</sub> ) <sub>2</sub> N	NO <sub>2</sub>	35	Chlorobenzene	255	[17]
7	(CH <sub>3</sub> ) <sub>2</sub> N	COOCH <sub>3</sub>	63	Toluene	227–228	[17]
8	Cl	NO <sub>2</sub>	68	Toluene	178–180	[18]
9	CH <sub>3</sub> O	NO <sub>2</sub>	72	Acetone	132–134	[19]
10	CH <sub>3</sub> O	CH <sub>3</sub>	82	Ethanol	167–169	[20]
11	CH <sub>3</sub> O	CN	76	Ethanol	149–151	[18]
12	CH <sub>3</sub> O	Cl	62	Ethanol/chloroform	177–178	[21]
13	Cl	CN	58	Dichloromethane	175–176	[22]
14	CH <sub>3</sub>	NO <sub>2</sub>	68	Ethanol	150–151	[22]
15	CH <sub>3</sub> O	COOCH <sub>3</sub>	78	Ethyl acetate	199–201	—
16	Br	COOCH <sub>3</sub>	76	Acetonitrile	171–173	—
17	CH <sub>3</sub>	CN	59	Ethanol	179–181	[22]
18	CH <sub>3</sub>	Cl	78	Ethanol	192–194	[22]
19	CH <sub>3</sub> O	NH <sub>2</sub>	83	—	167–168	—
20	Cl	NH <sub>2</sub>	80	—	199–200	—

Table 2

(a) Absorption maxima ( $\lambda_{max}$ ), molar extinction coefficient ( $\epsilon_{max}$ ) and fluorescence emission maxima ( $\lambda_{max}^0$ ) of *trans*-4,4'-*d*-substituted stilbenes in 2-butanone (MEK) and chlorobenzene (CB)

	X	Y	$\lambda_{max}$ (nm)		$\epsilon_{max}$ (M <sup>-1</sup> cm <sup>-1</sup> )		$\lambda_{max}^0$ (nm)	
			MEK	CB	MEK	CB	MEK	CB
1	(CH <sub>3</sub> ) <sub>2</sub> N	Br	362	368	33700	36080	445	428
2	(CH <sub>3</sub> ) <sub>2</sub> N	CN	384	394	19220	24400	504	479
3	(CH <sub>3</sub> ) <sub>2</sub> N	NO <sub>2</sub>	360	362	19970	33400	408	403
4	(CH <sub>3</sub> ) <sub>2</sub> N	Cl	360	366	34360	45250	447	425
5	(CH <sub>3</sub> ) <sub>2</sub> N	OCH <sub>3</sub>	352	356	15820	15860	418	402
6	(CH <sub>3</sub> ) <sub>2</sub> N	NO <sub>2</sub>	434	447	26960	26630	697	650
7	(CH <sub>3</sub> ) <sub>2</sub> N	COOCH <sub>3</sub>	382	388	28708	28100	498	478
8	Cl	NO <sub>2</sub>	352	356	26810	22600	—	397
9	CH <sub>3</sub> O	NO <sub>2</sub>	376	380	28500	26620	539	511
10	CH <sub>3</sub> O	CH <sub>3</sub>	328	326	21550	29890	374	370
11	CH <sub>3</sub> O	CN	338	334	34460	31820	419	397
12	CH <sub>3</sub> O	Cl	328	330	28300	21860	388	376
13	Cl	CN	328	330	38420	32370	386	380
14	CH <sub>3</sub>	NO <sub>2</sub>	—	376	—	26150	—	497
15	CH <sub>3</sub> O	COOCH <sub>3</sub>	338	—	37190	—	414	—
16	Br	COOCH <sub>3</sub>	328	—	21740	—	385	—
17	CH <sub>3</sub>	CN	—	334	—	28180	—	378
18	CH <sub>3</sub>	Cl	—	322	—	25010	—	364
19	CH <sub>3</sub> O	NO <sub>2</sub>	—	—	—	—	—	—
20	Cl	NO <sub>2</sub>	—	—	—	—	—	—

can be extended to various photophysical parameters of the excited molecules.

2. Solvent effects. Thermodynamically, solvation may be viewed along the same lines as substituent effects, the solvating molecules being equivalent to loosely attached substituents [14].

The quantitative structure–reactivity relationships based on a Hammett-like correlation with  $\sigma$ -values of substituents can indicate the photoisomerization mechanism for different substituted stilbenes. We assume that molecules lying on the same Hammett plot belong to the same reaction series, thus having the same *trans*–*cis* photoisomerization mechanism. Our results discussed below support this idea. This means that we can predict the photoisomerization mechanism of substituted stilbenes in arbitrary chosen media by considering the donor–acceptor properties of their substituents. Deviations from such linear relationships may be explained by additional effects which generate an additional series of reactions.

We carried out our studies of the substituent effects on the photoisomerization rate in four solvents: cyclohexane (CH), chlorobenzene (CB), methyl ethyl ketone (MEK), dimethylsulfoxide (DMSO). These solvents, except DMSO, do not interact specifically with the solute stilbene molecules. For polar substituted stilbenes one may expect an increasing sen-

sitivity of the isomerization rate to solvent effect, to the extent that it becomes more significant than the substituent effect.

	X	Y	$\lambda_{max}$ (nm)		$\lambda_{max}^0$ (nm)	
			CH	DMSO	CH	DMSO
1	(CH <sub>3</sub> ) <sub>2</sub> N	Br	358	358	391, 411	468
2	(CH <sub>3</sub> ) <sub>2</sub> N	CN	378	394	416, 445	537
3	(CH <sub>3</sub> ) <sub>2</sub> N	NO <sub>2</sub>	332, 352	368	386, 406	422
4	(CH <sub>3</sub> ) <sub>2</sub> N	Cl	356	358	389, 410	467
5	(CH <sub>3</sub> ) <sub>2</sub> N	OCH <sub>3</sub>	348	358	383, 402	435
6	(CH <sub>3</sub> ) <sub>2</sub> N	NO <sub>2</sub>	420	450	469, 498	—
7	(CH <sub>3</sub> ) <sub>2</sub> N	COOCH <sub>3</sub>	374	392	414, 442	543
8	Cl	NO <sub>2</sub>	—	—	—	—
9	CH <sub>3</sub> O	NO <sub>2</sub>	372	388	—	610
10	CH <sub>3</sub> O	CH <sub>3</sub>	306, 322	326	366	362
11	CH <sub>3</sub> O	CN	340	344	390	433
12	CH <sub>3</sub> O	Cl	310, 326	330	369	392
13	Cl	CN	326	330	370	387
14	CH <sub>3</sub>	NO <sub>2</sub>	356	372	—	551
15	CH <sub>3</sub> O	COOCH <sub>3</sub>	340	344	388	440
16	Br	COOCH <sub>3</sub>	332	333	373	397
17	CH <sub>3</sub>	CN	328	—	373	—
18	CH <sub>3</sub>	Cl	314, 318	—	360	—
19	CH <sub>3</sub> O	NO <sub>2</sub>	316, 332	350	386	427
20	Cl	NO <sub>2</sub>	336	356	392	455

## 2. Experimental details

### 2.1. Methods

#### 2.1.1. Steady-state measurements

Fluorescence emission spectra were recorded with an SLM Aminco–Bowman spectrofluorimeter after excitation near the absorption maxima ( $\lambda_{max}$ ), using typically a 4 nm slit width for both excitation and emission. Absorption and emission parameters of twenty *trans*-4,4'-disubstituted stilbenes (Table 1) are collected in Table 2. Quantum yields of fluorescence ( $\Phi_f$ ) were measured using *trans*-4-dimethylamino-4'-nitrostilbene in methylcyclohexane as the standard ( $\Phi_f^0 = 0.30$ ,  $\lambda_{max} = 420$  nm,  $\lambda_{max}^0 = 470$  nm) [2] including correction for absorption and intensity of the incident light, and are presented in Table 3. All the sample solutions were degassed with argon before the measurements.

#### 2.1.2. Time-resolved measurements

A picosecond time-resolved single photon counting apparatus was used to measure the fluorescence lifetime ( $\tau_f$ ). The

Table 3

Fluorescence quantum yield ( $\phi_f$ ) of *trans*-4,4'-disubstituted stilbenes in chlorobenzene (CB), 2-butanone (MEK) and dimethylsulfoxide (DMSO)

	X	Y	Quantum yield $\phi_f^{inh}$		
			CB	MEK	DMSO
1	(CH <sub>3</sub> ) <sub>2</sub> N	Br	0.044	0.018	0.030
2	(CH <sub>3</sub> ) <sub>2</sub> N	CN	0.015	0.024	0.109
3	(CH <sub>3</sub> ) <sub>2</sub> N	NH <sub>2</sub>	0.584	0.264	0.929
4	(CH <sub>3</sub> ) <sub>2</sub> N	Cl	0.047	0.024	0.051
5	(CH <sub>3</sub> ) <sub>2</sub> N	OCH <sub>3</sub>	0.167	0.069	0.249
6	(CH <sub>3</sub> ) <sub>2</sub> N	NO <sub>2</sub>	0.101	0.003	<0.001
7	(CH <sub>3</sub> ) <sub>2</sub> N	COOCH <sub>3</sub>	0.032	0.047	0.142
8	Cl	NO <sub>2</sub>	0.002	—	—
9	CH <sub>3</sub> O	NO <sub>2</sub>	0.084	0.114	0.003
10	CH <sub>3</sub> O	CH <sub>3</sub>	0.036	0.009	0.089
11	CH <sub>3</sub> O	CN	0.008	0.003	0.017
12	CH <sub>3</sub> O	Cl	0.016	0.004	0.041
13	Cl	CN	0.015	0.005	0.047
14	CH <sub>3</sub>	NO <sub>2</sub>	—	—	0.006
15	CH <sub>3</sub> O	COOCH <sub>3</sub>	—	—	0.027
16	Br	COOCH <sub>3</sub>	0.028	0.007	0.069
17	CH <sub>3</sub>	CN	0.009	—	—
18	CH <sub>3</sub>	Cl	0.020	—	—
19	CH <sub>3</sub> O	NH <sub>2</sub>	—	—	0.082
20	Cl	NH <sub>2</sub>	—	—	0.179

set-up consisted of a Ti-sapphire laser (Spectra-Physics, Tsunami laser pumped by a 10 W Beamlok Ar-ion laser) which was operated in its picosecond lasing mode (1 ps pulses at 82 MHz). The fundamental train of pulses was pulsed selected (Spectra-Physics, model 3980) to reduce its repetition rate down to typically 0.8–4.0 MHz and then passed through a doubling LBO crystal. The laser was tuned between 690 and 800 nm using the Spectra-Physics blue optics set, and the doubled frequency used for the excitation of the stilbenes was between 345 and 400 nm. The detection system consisted of a Hamamatsu 3809U 6 $\mu$  multi-channel plate (MCP). The fluorescence light was focused onto the entrance slit of the MCP after passing through a 1/8 m double monochromator (CVI model CM 112). The electronic processing of the signal was done by a combination of modular nim-bin units manufactured by Ortec, Tennelec and Phillips Scientific. The instrument function was typically 25 ps and was reduced to below 17 ps when 0.1 mm slits were put in front of the sample. The time resolution of the single photon counting set-up after data processing was below 3 ps in the 25 ns full-scale range of the time-to-amplitude converter (Tennelec 824). Typical counting rates were kept below 5 kHz. The number of counts was between 4k and 10k at the peak channel and these were collected by the Tennelec PCA3 Card. Further signal processing and data analysis was done by personal computers.

The lifetimes of the first excited singlet state ( $\tau_f$ ) in four solvents of different polarities (CH, CB, MEK, DMSO) are presented in Table 4. An example of the time-resolved fluorescence decay profile is shown in Fig. 2.

Table 4

Excited state lifetime of *trans*-4,4'-disubstituted stilbenes in cyclohexane (CH), chlorobenzene (CB), 2-butanone (MEK) and dimethylsulfoxide (DMSO)

	X	Y	$\sigma_x - \sigma_y$	Fluorescence lifetime $\tau_f$ (ps)			
				CH	CB	MEK	DMSO
1	(CH <sub>3</sub> ) <sub>2</sub> N	Br	1.06	168	315	206	225
2	(CH <sub>3</sub> ) <sub>2</sub> N	CN	1.49	75	251	330	900
3	(CH <sub>3</sub> ) <sub>2</sub> N	NH <sub>2</sub>	0.17	1170	1075	585	1183
4	(CH <sub>3</sub> ) <sub>2</sub> N	Cl	1.06	165	325	243	597
5	(CH <sub>3</sub> ) <sub>2</sub> N	OCH <sub>3</sub>	0.56	447	609	444	870
6	(CH <sub>3</sub> ) <sub>2</sub> N	NO <sub>2</sub>	1.61	939	1830	126	—
7	(CH <sub>3</sub> ) <sub>2</sub> N	COOCH <sub>3</sub>	1.28	144	298	549	1353
8	Cl	NO <sub>2</sub>	0.55	—	66	—	—
9	CH <sub>3</sub> O	NO <sub>2</sub>	1.05	—	1253	560	1527
10	CH <sub>3</sub> O	CH <sub>3</sub>	0.10	207	153	78	117
11	CH <sub>3</sub> O	CN	0.93	20	24	15	45
12	CH <sub>3</sub> O	Cl	0.50	69	49	32	64
13	Cl	CN	0.43	60	59	38	75
14	CH <sub>3</sub>	NO <sub>2</sub>	0.95	—	67	1005	—
15	CH <sub>3</sub> O	COOCH <sub>3</sub>	0.72	48	—	21	66
16	Br	COOCH <sub>3</sub>	0.22	15	—	61	108
17	CH <sub>3</sub>	CN	0.83	111	30	—	—
18	CH <sub>3</sub>	Cl	0.40	22	68	—	—
19	CH <sub>3</sub> O	NH <sub>2</sub>	0.39	51	—	—	99
20	Cl	NH <sub>2</sub>	0.89	531	—	—	207

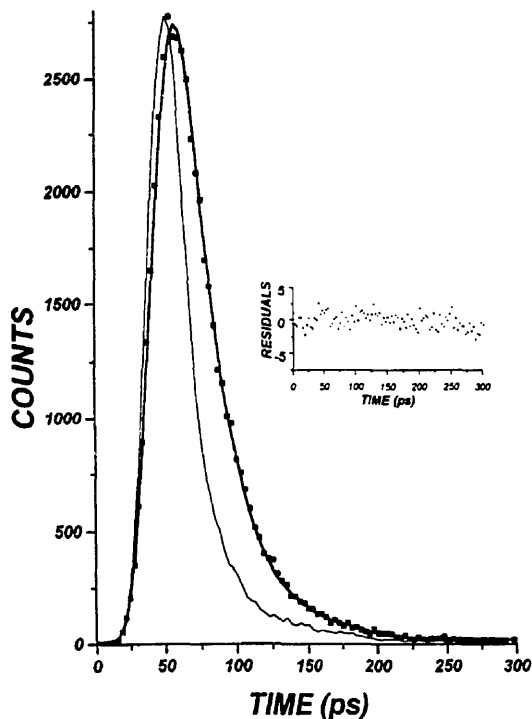


Fig. 2. Time-resolved fluorescence decay profile of 4-methoxy-4'-cyano-stilbene in methyl ethyl ketone (concentration 8  $\mu$ M). The instrument function (solid line) is 20 ps, and the experimental data (dots) were fitted after convolution by  $\tau_f = 15$  ps with  $\chi^2 = 0.8$ .

## 2.2. Materials

### 2.2.1. Reagents and solvents

The following commercial solvents and reagents were used: methylcyclohexane (spectrophotometric grade, Merck), toluene, methanol, petroleum ether (40–60°), acetone, isopropanol, 1,4-dioxane, ethanol, chloroform, ethyl acetate, dichloromethane (chemically pure, Frutarom, Israel), xylene (spectrophotometric grade, Merck), 2-butanone (spectrophotometric grade, Aldrich), chlorobenzene (spectrophotometric grade, Merck), triphenylphosphine (Merck), LiOCH<sub>3</sub> (1 M solution in absolute methanol, Aldrich), carbon tetrachloride (analytical, Frutarom, Israel), benzoyl peroxide (Aldrich), *N*-bromosuccinimide (Merck), 4-nitrobenzaldehyde, 4-methoxybenzaldehyde (4-anisaldehyde), 4-chlorobenzaldehyde, 4-dimethylaminobenzaldehyde, 4-tolualdehyde, 4-bromobenzyl bromide, 4-methoxybenzyl chloride, 4-toluenitrile, 4-nitrotoluene (Aldrich).

### 2.2.2. Synthesis of stilbene derivatives

The following substituted stilbenes were prepared by the procedure outlined elsewhere [17]: *trans*-4-dimethylamino-4'-nitrostilbene, *trans*-4-dimethylamino-4'-chlorostilbene, *trans*-4-dimethylamino-4'-aminostilbene. <sup>1</sup>H NMR spectra were taken at 298 K on a 500 MHz Bruker Fourier transform spectrometer, equipped with a DMX Avance system and Bruker UXNMR program with Me<sub>4</sub>Si as the internal standard on 10% w/v solutions in CDCl<sub>3</sub> or DMSO-*d*<sub>6</sub>. Melting points were determined on a Kofler melting apparatus and are uncorrected. UV absorption spectra were recorded on a Hewlett-Packard UV-visible 200HP spectrophotometer. Preparative column chromatography was performed with silica gel 60 (Merck, 230–400 mesh ASTM).

*4*-substituted benzyl bromides. 4-cyanobenzyl bromide and 4-nitrobenzyl bromide were prepared from the corresponding 4-substituted toluenes by bromination with *N*-bromosuccinimide in dry carbon tetrachloride in the presence of benzoyl peroxide [16]. Methyl  $\alpha$ -bromo-4-toluate was prepared by a modified method of Fuson and Cooke [23].

*Preparation of triphenylphosphonium salts.* The required triphenylphosphonium salt was prepared from the corresponding 4-substituted benzyl bromide and triphenylphosphine in toluene [16]. In short, 10 mmol of benzyl halide and 12 mmol of triphenylphosphine were dissolved in 50 ml of toluene, and the reaction mixture was heated at 80–90 °C for 6–7 h. The precipitated salt was collected and washed twice with acetone and petroleum ether and then dried in a vacuum oven at 140 °C overnight. All of the salts were purified by recrystallization and yielded satisfactory melting points compared with the literature values [16]. 4-(carbomethoxybenzyl)triphenylphosphonium bromide and 4-(bromobenzyl)triphenylphosphonium bromide were subjected to elemental and <sup>1</sup>H NMR analyses which proved their chemical purity and structural identity.

*Preparation of substituted stilbenes.* 10 mmol of the corresponding triphenylphosphonium salt and 11 mmol of the 4-substituted benzaldehyde were dissolved in 25 ml of absolute methanol. 25 ml of 0.4 M lithium methoxide solution in absolute methanol was added, and the reaction mixture was stirred intensively at room temperature for 10–15 min. The resulting solution was left to stand overnight at room temperature to provide the precipitation of the product. The precipitated crystals of the *trans*-isomer were collected and recrystallized (Table 1). The mother liquor containing mostly the *cis*-isomer was concentrated in a vacuum rotary evaporator, and the precipitated crystals of the *cis*-isomer were collected and treated with the iodine solution in xylene to promote the *cis* to *trans* back isomerization and formation of the required *trans*-isomer [16]. All these compounds were purified by column chromatography on silica gel and recrystallization. The structures were confirmed by <sup>1</sup>H NMR and mass spectroscopy; melting points were in a good agreement with the literature values (Table 1).

All of the new stilbenes, *trans*-4-dimethylamino-4'-carbomethoxystilbene, *trans*-4-carbomethoxy-4'-bromostilbene and *trans*-4-carbomethoxy-4'-methoxystilbene, were subjected to elemental and <sup>1</sup>H NMR analyses, and mass spectroscopy.

*Trans*-4-dimethylamino-4'-carbomethoxystilbene. <sup>1</sup>H NMR (CDCl<sub>3</sub>):  $\delta$  3.00 (s, 6H Me<sub>2</sub>N);  $\delta$  3.91 (s, 3H MeOOC); CH=CH AB pattern  $\delta$  6.92 (d, vinyl 1H),  $\delta$  7.16 (d, vinyl 1H); 4-Me<sub>2</sub>N-Ar AA'XX' pattern  $\delta$  6.71 (d, 2H: H3, H5),  $\delta$  7.43 (d, 2H: H2, H6); 4-MeOOC-Ar AA'XX' pattern  $\delta$  7.51 (d, 2H: H2', H6'),  $\delta$  7.98 (d, 2H: H3', H5'). Analysis found: C, 77.12; H, 6.89; N, 4.91. C<sub>18</sub>H<sub>19</sub>NO<sub>2</sub> calculated: C, 76.84; H, 6.81; N, 4.98.

*Trans*-4-carbomethoxy-4'-bromostilbene. <sup>1</sup>H NMR (CDCl<sub>3</sub>):  $\delta$  3.91 (s, 3H, MeOOC); CH=CH AB pattern  $\delta$  6.60 (d, vinyl 1H),  $\delta$  7.09 (d, vinyl 1H); 4-Br-Ar AA'BB' pattern  $\delta$  7.35 (d, 2H: H3, H5),  $\delta$  7.40 (d, 2H: H2, H6); 4-MeOOC-Ar AA'XX' pattern  $\delta$  7.54 (d, 2H: H2', H6'),  $\delta$  7.97 (d, 2H: H3', H5'). Analysis found: C, 60.28; H, 4.19; Br, 25.44. C<sub>16</sub>H<sub>13</sub>BrO<sub>2</sub> calculated: C, 60.59; H, 4.13; Br, 25.19.

*Trans*-4-carbomethoxy-4'-methoxystilbene. <sup>1</sup>H NMR (CDCl<sub>3</sub>):  $\delta$  3.85 (s, 3H, MeO);  $\delta$  3.91 (s, 3H, MeOOC); CH=CH AB pattern  $\delta$  7.00 (d, vinyl 1H),  $\delta$  7.18 (d, vinyl 1H); 4-MeO-Ar AA'XX' pattern  $\delta$  6.87 (2, 2H: H3, H5),  $\delta$  7.46 (d, 2H: H2, H6); 4-MeOOC-Ar AA'XX' pattern  $\delta$  7.54 (d, 2H: H2', H6'),  $\delta$  8.01 (d, 2H: H3', H5'). Analysis found: C, 75.82; H, 6.36. C<sub>17</sub>H<sub>17</sub>O<sub>3</sub> calculated: C, 75.49; H, 6.40. Mass spectroscopy: 269 M<sup>+</sup> 100%, 238 [M<sup>+</sup>-OCH<sub>3</sub>] 10%.

## 3. Results and discussion

In this study we have measured the fluorescence lifetime  $\tau_f$  and quantum yield  $\Phi_f$  of various *trans*-stilbene derivatives. Generally speaking, the  $\tau_f$  may be expressed as

$$\tau_f = (k_r + k_{nr} + k_{t \rightarrow c})^{-1} \quad (1)$$

where  $k_r$  and  $k_{nr}$  are the radiative and non-radiative decay rate constants respectively and  $k_{t \rightarrow c}$  is the *trans*–*cis* photoisomerization rate constant.

In most cases studied  $k_{t \rightarrow c} \gg k_r$  and  $k_{t \rightarrow c} \gg k_{nr}$ , so to a good approximation  $\tau_1 \approx (k_{t \rightarrow c})^{-1}$ , and

$$\Phi_1 = k_r / (k_r + k_{nr} + k_{t \rightarrow c}) \approx k_r / k_{t \rightarrow c} \quad (2)$$

So, both  $\tau_1$  and  $\Phi_1$  are mainly determined by the *trans*–*cis* photoisomerization rate.

A commonly accepted model for *trans*–*cis* isomerization of stilbene assumes a one-dimensional reaction coordinate  $\theta$ , which is the torsion (twist) angle about the olefinic double bond [2–5,12] (Fig. 1). The transition state allowed for the *trans*–*cis* isomerization in the excited singlet state is expected to be polarizable and involve zwitterionic structures which lower the barrier to the torsional motion, facilitating the isomerization reaction.

The charge separation associated with this reaction may be stabilized intramolecularly by polar 4,4'-substituents on the aromatic rings of stilbenes, or externally by polar solvents. The former is a Hammett-like mechanism, while the latter involves media-stabilizing effects on the transition state. Assuming the dielectric response of the solvent is fast compared with the twisting motion, both effects may be described quantitatively in terms of free-energy relationships. Therefore, solvent polarity affects the excited energy level of the

twisted  $^1p^*$  intermediate (TSI) by stabilizing its separated charges and consequently lowers the intrinsic barrier to  $^1t^* \rightarrow ^1p^*$  torsional distortion.

For *trans*-4,4'-disubstituted stilbenes without strong donor–acceptor substituents one expects  $k_{t \rightarrow c}$  to increase with solvent polarity and with the ability of the 4,4'-substituents to stabilize the charge separation in the excited state. A good measure for the substituent effect is the difference between the Hammett  $\sigma$ -values of the 4,4'-substituents. In such cases the energy of the more polar 'phantom' state,  $^1p^*$ , is lowered in comparison with the energy of the *trans*-singlet state,  $^1t^*$ , so the activation free energy for the *trans*–*cis* photoisomerization is reduced and  $k_{t \rightarrow c}$  increases.

In contrast, strong donor–acceptor substituents are able to stabilize the  $^1t^*$  compared with the  $^1p^*$  state, so the activation energy increases and the isomerization rate decreases (Fig. 3). A  $^1p^*$  state of low polarity is in fact predicted by quantum-chemical calculations for strong donor–acceptor stilbenes, whereas for non-polar stilbenes a very highly polar  $^1p^*$  state is expected [24,25]. This switching from high to low polarity of the  $^1p^*$  state is the result of the biradicaloid nature of this state, which undergoes 'sudden polarization' [26].

Figs. 4 and 5 demonstrate the linear dependence of  $\log(1/\tau_1)$  and  $\log\Phi_1$  on  $(\sigma_X - \sigma_Y)$ , where X and Y denote the two *para*-substituents at the opposite 4 and 4'-phenyl ring positions. Inspection of Figs. 4 and 5 shows that apart from stilbene derivatives which include the strong donor dimethylamino substituent at one of the *para*-positions, all

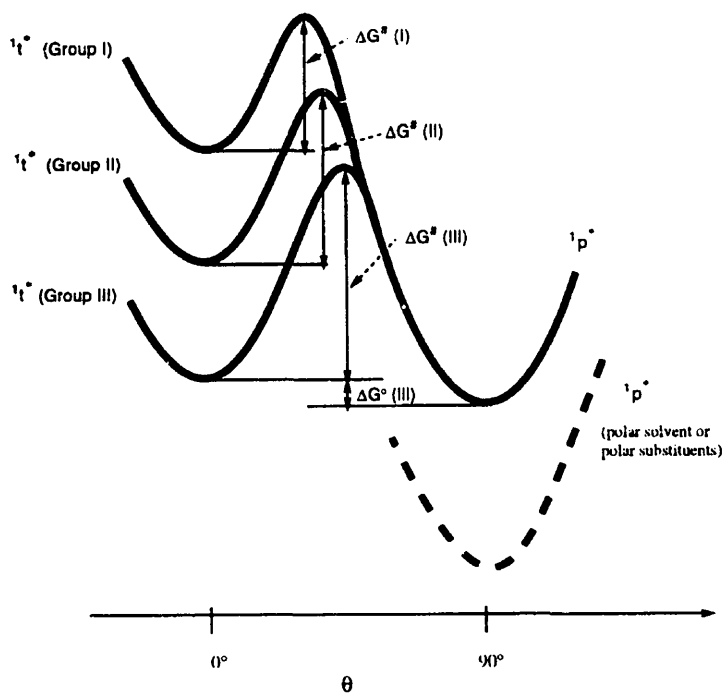
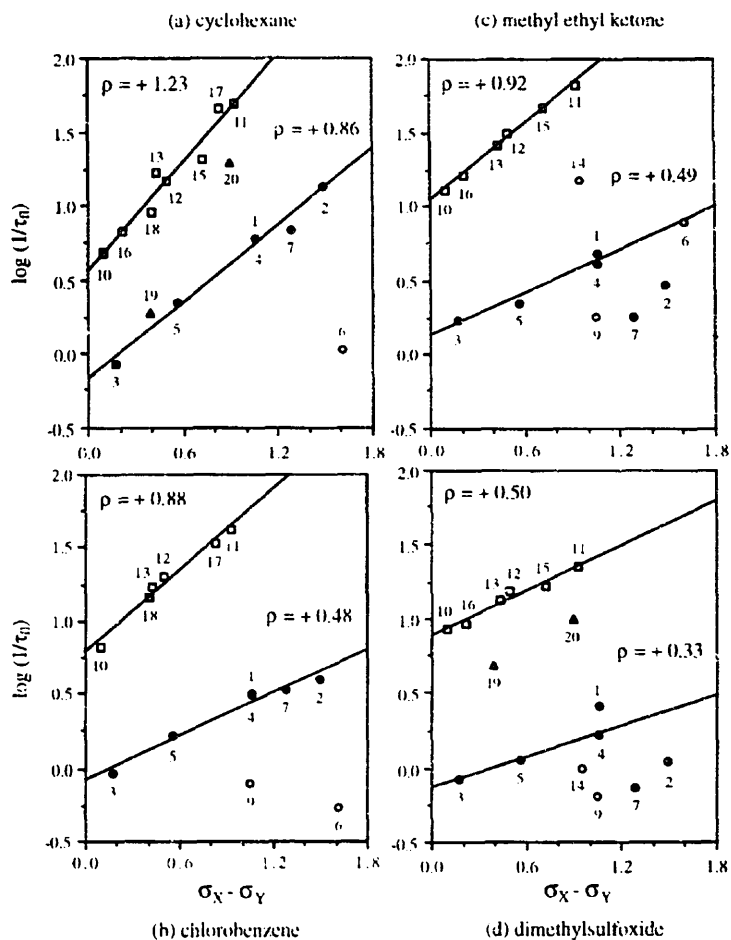


Fig. 3. Schematic representation of potential energy curves of the excited singlet state  $^1t^*$  (left) and excited singlet twisted state  $^1p^*$  (right) for the different groups of *trans*-4,4'-distributed stilbenes in different polar solvents.



- |                                     |                                       |                                    |                                 |
|-------------------------------------|---------------------------------------|------------------------------------|---------------------------------|
| 1 - $(\text{CH}_3)_2\text{N,Br}$    | 6 - $(\text{CH}_3)_2\text{N,NO}_2$    | 11 - $\text{CH}_3\text{O,CN}$      | 16 - $\text{Br,COOCH}_3$        |
| 2 - $(\text{CH}_3)_2\text{N,CN}$    | 7 - $(\text{CH}_3)_2\text{N,COOCH}_3$ | 12 - $\text{CH}_3\text{O,Cl}$      | 17 - $\text{CH}_3\text{,CN}$    |
| 3 - $(\text{CH}_3)_2\text{N,NH}_2$  | 8 - $\text{Cl,NO}_2$                  | 13 - $\text{Cl,CN}$                | 18 - $\text{CH}_3\text{,Cl}$    |
| 4 - $(\text{CH}_3)_2\text{N,Cl}$    | 9 - $\text{CH}_3\text{O,NO}_2$        | 14 - $\text{CH}_3\text{,NO}_2$     | 19 - $\text{CH}_3\text{O,NH}_2$ |
| 5 - $(\text{CH}_3)_2\text{N,OCH}_3$ | 10 - $\text{CH}_3\text{O,CH}_3$       | 15 - $\text{CH}_3\text{O,COOCH}_3$ | 20 - $\text{Cl,NH}_2$           |

Fig. 4. Plot of the fluorescence decay rate of the  $1^{\text{st}}$  state vs. Hammett  $\sigma$ -constant difference ( $\sigma_X - \sigma_Y$ ) for *trans*-4,4'-disubstituted stilbenes. The four experimental series are (a) in CH. (b) in CB. (c) in MEK, and (d) in DMSO. Concentration of the samples was 8  $\mu\text{M}$ . ( $\sigma_X - \sigma_Y$ ) was calculated as the difference between the  $\sigma$ -constants of the two 4,4'-positioned substituents (X and Y) taking in account their relative sign. The group I stilbenes are designated by open squares, and the group II stilbenes by dots. The 4-nitro-derivatives deviating from the linear dependence are designated by open circles. Lifetime ( $\tau_n$ ) is given in nanoseconds (ns).

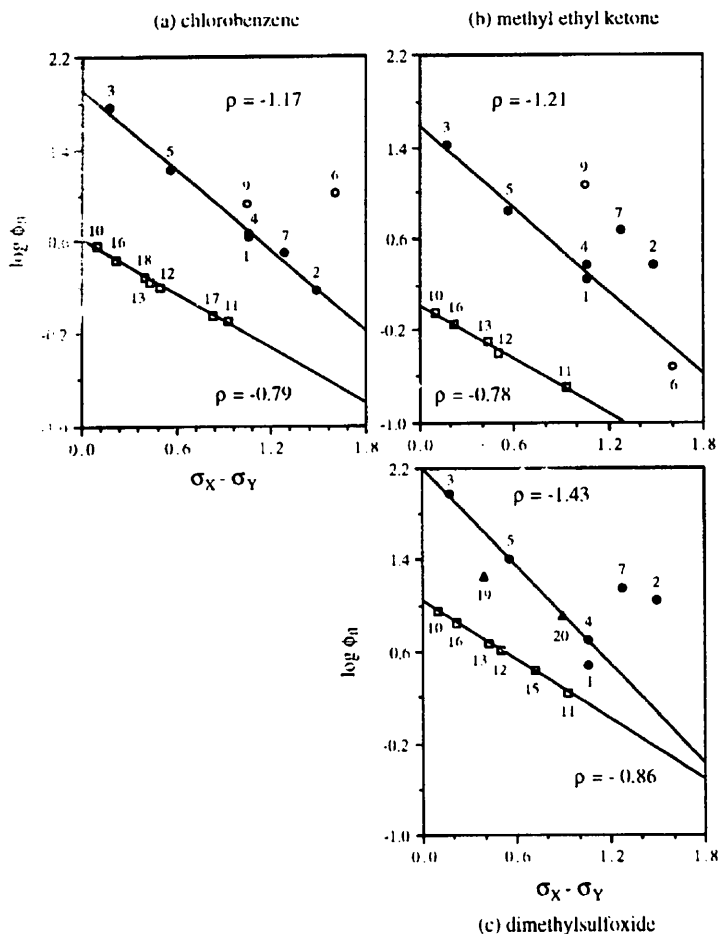
other substituted stilbenes follow the same trends of reactivity.

Moving from the less polar solvents to the polar solvents, the photoisomerization rate increases with the polarity of the solvent, and the slope of the linear dependence ( $\rho$ -value) between ( $\sigma_X - \sigma_Y$ ) and  $\log(1/\tau_1)$  decreases. This shows that solvent polarity levels off the intramolecular effect of polar substituents. When one of the two substituents is the

$(\text{CH}_3)_2\text{N}$  group, the photoisomerization rate decreases considerably but usually follows the general trends described above with a smaller  $\rho$ -value.

The situation may be summarized with the aid of Fig. 6, as follows.

*Group I* stilbenes (*trans*-4,4'-disubstituted stilbenes without strong donor-acceptor substituents) have the charges separated and localized around the zwitterion in the excited



1 - (CH <sub>3</sub> ) <sub>2</sub> N,Br	6 - (CH <sub>3</sub> ) <sub>2</sub> N,NO <sub>2</sub>	11 - CH <sub>3</sub> O,CN	16 - Br,COOCH <sub>3</sub>
2 - (CH <sub>3</sub> ) <sub>2</sub> N,CN	7 - (CH <sub>3</sub> ) <sub>2</sub> N,COOCH <sub>3</sub>	12 - CH <sub>3</sub> O,Cl	17 - CH <sub>3</sub> ,CN
3 - (CH <sub>3</sub> ) <sub>2</sub> N,NH <sub>2</sub>	8 - Cl,NO <sub>2</sub>	13 - Cl,CN	18 - CH <sub>3</sub> ,Cl
4 - (CH <sub>3</sub> ) <sub>2</sub> N,Cl	9 - CH <sub>3</sub> O,NO <sub>2</sub>	14 - CH <sub>3</sub> ,NO <sub>2</sub>	19 - CH <sub>3</sub> O,NH <sub>2</sub>
5 - (CH <sub>3</sub> ) <sub>2</sub> N,OCCH <sub>3</sub>	10 - CH <sub>3</sub> O,CH <sub>3</sub>	15 - CH <sub>3</sub> O,COOCH <sub>3</sub>	20 - Cl,NH <sub>2</sub>

Fig. 5. Plot of the fluorescence quantum yield vs. Hammett  $\sigma$ -constant difference ( $\sigma_X - \sigma_Y$ ) for *trans*-4,4'-disubstituted stilbenes. The three experimental series are (a) in CB, (b) in MEK and (c) in DMSO. Concentration of the samples was 8  $\mu$ M. ( $\sigma_X - \sigma_Y$ ) was calculated as the difference between the  $\sigma$ -constants of the two 4,4'-positioned substituents (X and Y) taking in account their relative sign. The group I stilbenes are designated by open squares, and the group II stilbenes by dots. The 4-nitro-derivatives deviating from the linear dependence are designated by open circles. Quantum yields ( $f_n$ ) are given in per cent.

singlet  $^1t^*$  state. These separated charges are expected to be considerably localized in the  $^1t^*$  state and, therefore, undergo the fast  $^1t^* \rightarrow ^1p^*$  reaction with a high rate constant,  $1/\tau_r$ . For such stilbenes, both polar substituents and polar solvents are expected to stabilize the twisted intermediate  $^1p^*$  compared with the less polar  $^1t^*$  state. So, an increase in the isomerization rate is expected and indeed observed for both cases.

The Hammett-like correlation is excellent in all investigated solvents. In this case, with decreasing  $\rho$ -values as the polarity of the solvent increases, both quantum yield and

lifetime measurements have similar substituent dependence, indicating a similar isomerization mechanism along the group. This means that in the case of non-polar or slightly polar stilbenes without strong donor–acceptor substituents, the primary effect of solvent polarity will be on the transition-state energy, and a singlet *trans*–*cis* photoisomerization pathway similar to that occurring with the parent stilbene molecule may be assumed. This may imply that the twisted intermediate  $^1p^*$  needs to assume a specific structure about the twisted double bond regardless of the chemical nature of the substituents.



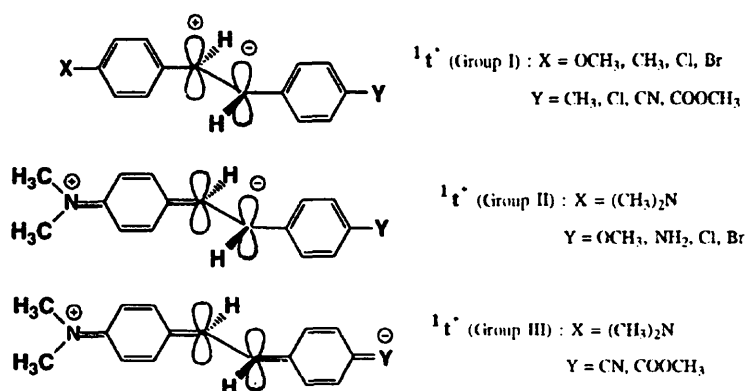


Fig. 6. Classification of *trans*-4,4'-disubstituted stilbenes according to the substituent effect on the excited singlet  ${}^1t^*$  state.

*Group II* stilbenes have the strong donor substituent (CH<sub>3</sub>)<sub>2</sub>N in the *para*-position on the aromatic ring. They are characterized by a large red shift in both the absorption and the fluorescence spectra of the *trans*-stilbenes. The (CH<sub>3</sub>)<sub>2</sub>N group participates in charge delocalization in the  ${}^1t^*$ -state, thus stabilizing it in comparison with the  ${}^1p^*$ -state. This causes an increase in the  ${}^1t^* \rightarrow {}^1p^*$  activation energy and a drop in the transition rate with a low rate constant,  $1/\tau_1$ .

Polar *para*-substituents on the second ring cause similar electronic-inductive effects as in the case of the first group stilbenes, but these effects are of smaller amplitudes (smaller  $\rho$ -value means less sensitivity of the transition state to substituent effects). This means that the stabilizing effect of the (CH<sub>3</sub>)<sub>2</sub>N group on the  ${}^1t^*$  state is more pronounced than the polar stabilization of the  ${}^1p^*$  state.

As can be seen in Figs. 4 and 5, a change of solvent affects the two stilbene families by an almost identical amount. Comparison between quantum yield and lifetime measurements of the second stilbene group indicates that, contrary to group I, the quantum yields in group II are much more sensitive (larger  $\rho$ -value) to substitution than the lifetimes. This means that substitution must also affect the non-radiative and the radiative channels of group II stilbenes. Therefore, in group II the *trans-cis* photoisomerization mechanism is more complex than that assumed for group I and includes a combination of singlet, triplet and intramolecular charge transfer pathways and is dependent on the specific nature of the *para*-substituent.

For example, 4-dimethylamino-4'-bromostilbene deviates from the linear Hammett plot of both the fluorescence lifetime and quantum yield in the relative polar MEK and DMSO solvents. In this case, the non-radiative decay pathway which takes over [6,8] is responsible for this deviation.

The two following stilbenes with strong donor-acceptor pairs of substituents (D  $\equiv$  (CH<sub>3</sub>)<sub>2</sub>N, A  $\equiv$  CN, COOCH<sub>3</sub>), so called 'push-pull' stilbenes, *trans*-4-dimethylamino-4'-cyanostilbene (DACS) and a new *trans*-4-dimethylamino-4'-carbomethoxystilbene (DACMS), deviate from the linear dependence of  $\log(1/\tau_1)$  and  $\log\Phi_f$  on the Hammett  $\sigma$ -con-

stants only in polar media and may be considered separately (conveniently designated as 'group III', although these molecules do not necessarily conform to the same *trans-cis* photoisomerization pathway). These derivatives exhibit very large red shifts, compared with groups I and II and fall below the linear Hammett plot. The formation of a twisted intramolecular charge transfer (TICT) structure in the excited singlet state may be responsible for this behavior [27–30].

The presence of two time-resolved emission bands (from the  ${}^1t^*$  and TICT states respectively) was reported for DACS where the existence of a TICT state was assumed [30,24]. We have also observed two emissive bands in DACS and DACMS dissolved in MEK and DMSO using high-resolution picosecond time-resolved measurements. This supports but does not prove the existence of a TICT state in DACS and DACMS. A subsequent publication will be devoted to this phenomenon.

The deviation of the 4-nitro-substituted stilbenes from the linear Hammett-like behavior is more complex and is attributed to a specific interaction of the nitro-group which quenches the charge-transfer state emission. In these cases a non-emissive TICT state was assumed [25,26].

#### 4. Conclusion

In this study we show that the effect of 4,4'-substitutions on the isomerization reaction of *trans*-stilbenes may be correlated by their corresponding Hammett  $\sigma$ -values.

Donor-acceptor pairs of 4,4'-substituents usually increase the rate of the  ${}^1t^* \rightarrow {}^1p^*$  transition owing to the stabilization of the more polar  ${}^1p^*$  state. Solvent polarity affects this transition in a similar way, so the rate of the *trans-cis* isomerization reaction is increased by both polar solvents and polar substituents. A second group of substituents tends to participate in charge delocalization in the  ${}^1t^*$  state. This electronic resonance interaction in the  ${}^1t^*$  state destabilizes the transition to the  ${}^1p^*$  state and retards the isomerization reaction. Our study also supports the existence of a third group of substit-

uents which cause the formation of an additional charge transfer state appearing below the  $^1t^*$  state. The transition from this state to the  $^1p^*$  state is much slower than the transition from the  $^1t^*$  state. The charge transfer state becomes important in cases of strong donor–acceptor interactions and manifests itself by a large red shift in both the absorption and the emission spectra. It also causes large deviations from the linear Hammett plots. These two effects may help in identifying the appearance of a new emitting state which complicates the photophysical behavior of substituted *trans*-stilbenes.

### Acknowledgements

The authors wish to thank Professor Jack Saltiel for his valuable comments and Vladimir Khodorkovsky for his advice in organic synthesis. Ehud Pines thanks the German–Israeli James Franck Program on Laser–Matter Interactions for its financial support.

### References

- [1] (a) J. Saltiel, J.D. Agostino, E.D. Megarity, L. Metts, K.R. Neuberger, M. Wrighton, O.C. Zalariou, in O.L. Chapman (ed.), *Organic Photochemistry*, Vol. 3, Marcel Dekker, New York, 1973, p. 1. (b) J. Saltiel, Y.-P. Sun, in H. Durr, H. Bouas-Laurent (eds.), *Photochromism, Molecules and Systems*, Elsevier, Amsterdam, 1990, p. 64.
- [2] D.H. Waldek, *Chem. Rev.*, 91 (1991) 415.
- [3] N.S. Park, D.H. Waldek, *J. Chem. Phys.*, 91 (1989) 943.
- [4] H. Meier, *Angew. Chem.*, 31 (1992) 1399.
- [5] (a) J. Saltiel, A.S. Waller, D.F. Sears, E.A. Hoburg, D.M. Zeglinski, D.H. Waldek, *J. Chem. Phys.*, 98 (1994) 10689. (b) J. Saltiel, Y. Zhang, F.S. Donald, *J. Am. Chem. Soc.*, 118 (1996) 2811. (c) J. Saltiel, Y.-P. Sun, *J. Phys. Chem.*, 93 (1989) 6246. (d) J. Saltiel, A.S. Waller, D.F. Sears, *J. Am. Chem. Soc.*, 115 (1993) 2453.
- [6] (a) H. Gruen, H. Görner, *J. Phys. Chem.*, 93 (1989) 7144. (b) H. Görner, H. Kuhn, *J. Adv. Photochem.*, 19 (1995) 1.
- [7] (a) S.K. Kim, G.R. Fleming, *J. Phys. Chem.*, 92 (1988) 2168. (b) S.H. Courtney, G.R. Fleming, *J. Chem. Phys.*, 83 (1985) 215. (c) G.R. Fleming, S.H. Courtney, M.W. Balk, *J. Stat. Phys.*, 42 (1986) 83.
- [8] D. Gegiou, K.A. Muszkat, E. Fischer, *J. Am. Chem. Soc.*, 90 (1968) 3907.
- [9] R.M. Hochstrasser, *Pure Appl. Chem.*, 52 (1980) 2683.
- [10] D. Schulte-Frohlinde, H. Blume, H. Gusten, *J. Phys. Chem.*, 66 (1962) 2486.
- [11] S. Malkin, E. Fisher, *J. Phys. Chem.*, 68 (1964) 1153.
- [12] J. Saltiel, *J. Am. Chem. Soc.*, 89 (1967) 1036; 90 (1968) 6394.
- [13] E.S. Lewis, *Linear Free-Energy Relationships*. In C.F. Bernasconi (ed.), *Investigation of Rates and Mechanisms of Reactions*, Vol. IV, *Techniques in Chemistry Series*, Wiley, New York, 1986, Part I, 4th edn.
- [14] J.E. Leffler, E. Grunwald, in *Rates and Equilibria of Organic Reactions*, Wiley, New York, London, 1963.
- [15] M. Syz, H. Zollinger, *Helv. Chim. Acta*, 48 (1965) 517.
- [16] G. Manecke, S. Lütke, *Chem. Ber.*, 103 (1970) 700.
- [17] G.I. Likhtenshtein, B. Rizak, V. Papper, B. Uzan, I. Fishov, D. Gill, A.H. Parola, *J. Biochem. Biophys. Methods*, 33 (1996) 117.
- [18] H. Meerwein, E. Büchner, K. Van Emster, *J. Prakt. Chem.*, 152 (1939) 259.
- [19] R. Ketchani, L. Martinelli, *J. Org. Chem.*, 27 (1962) 4666.
- [20] T. Troxler, M.R. Topp, B.S. Metzger, L.H. Spangler, *Chem. Phys. Lett.*, 238 (1995) 313.
- [21] R. Neher, K. Miescher, *Helv. Chem. Acta*, 29 (1946) 460.
- [22] P. Pfeiffer, *Ber. Dtsch. Chem. Ges.*, 48 (1915) 1777.
- [23] R.C. Fuson, H.G. Cooke, *J. Am. Chem. Soc.*, 62 (1940) 1180.
- [24] R. Lapouyade, K. Czeschka, W. Majenz, W. Rettig, E. Gilabert, C. Rulliere, *J. Phys. Chem.*, 96 (1992) 9643.
- [25] R. Lapouyade, A. Kuhn, J.-F. Letard, W. Rettig, *Chem. Phys. Lett.*, 208 (1993) 48.
- [26] J. Michl, V. Bonacic-Koutecky, *Electronic Aspects of Organic Photochemistry*, Wiley, New York, 1990.
- [27] (a) E. Gilabert, R. Lapouyade, C. Rulliere, *Chem. Phys. Lett.*, 145 (1988) 262. (b) D.M. Zeglinski, D.H. Waldeck, *J. Phys. Chem.*, 92 (1988) 692.
- [28] W. Rettig, B. Strehmal, W. Majenz, *Chem. Phys.*, 173 (1993) 525.
- [29] A. Klock, W. Rettig, *Pol. J. Chem.*, 67 (1993) 1375.
- [30] W. Rettig, W. Majenz, *Chem. Phys. Lett.*, 154 (1989) 335.